Biochimica et Biophysica Acta 1793 (2009) 1325–1333

Contents lists available at ScienceDirect

Biochimica et Biophysica Acta

journal homepage: www.elsevier.com/locate/bbamcr

Caveolin-2 regulation of STAT3 transcriptional activation in response to insulin

Hayeong Kwon [a], Kyuho Jeong [a], Eun Mi Hwang [b], Jae-Yong Park [b], Seong-Geun Hong [b], Wan-Sung Choi [c], Yunbae Pak [a,*]

[a] Department of Biochemistry, Division of Applied Life Science (BK21 Program), PMBBRC, Gyeongsang National University, Jinju 660-701, Republic of Korea
[b] Department of Physiology, Institute of Health Science, Medical Research Center for Neural Dysfunction, Gyeongsang National University, Jinju 660-701, Republic of Korea
[c] Department of Anatomy, Institute of Health Science, Medical Research Center for Neural Dysfunction, Gyeongsang National University, Jinju 660-701, Republic of Korea

ARTICLE INFO

Article history:
Received 24 January 2009
Received in revised form 1 April 2009
Accepted 29 April 2009
Available online 7 May 2009

Keywords:
pY19-Caveolin-2
pY27-Caveolin-2
pY705-STAT3
pS727-STAT3
Insulin
Caveolin-2 siRNA
Caveolin-2 tyrosine variant mutant
STAT3 transcriptional activation

ABSTRACT

The regulatory function of caveolin-2 in signal transducer and activator of transcription 3 (STAT3) signaling by insulin was investigated. Insulin-induced increase in phosphorylation of STAT3 was reduced by caveolin-2 siRNA. Mutagenesis studies identified that phosphorylation of tyrosines 19 and 27 on caveolin-2 is required for the STAT3 activation. Caveolin-2 Y27A mutation decreased insulin-induced phosphorylation of STAT3 interacting with caveolin-2. pY27-Caveolin-2 was required for nuclear translocation of pY705-STAT3 in response to insulin. In contrast, caveolin-2 Y19A mutation influenced neither the phosphorylation of STAT3 nor nuclear translocation of pY705-STAT3. pY19-Caveolin-2, however, was essential for insulin-induced DNA binding of pS727-STAT3 and STAT3-targeted gene induction in the nucleus. Finally, insulin-induced transcriptional activation of STAT3 depended on phosphorylation of both 19 and 27 tyrosines. Together, our data reveal that phosphotyrosine-caveolin-2 is a novel regulator for transcriptional activation of STAT3 in response to insulin.

1. Introduction

Signal transducers and activators of transcription (STATs) are cytoplasmic proteins that selectively activate nuclear gene transcription [1,2]. The activation of STAT proteins involves phosphorylation, dimerization, nuclear translocation and activation of transcription by binding to DNA-response elements of target genes [2,3]. STAT proteins have a Src-homology domain 2 (SH2) near the C-terminus. The SH2 domain of STATs mediates the selective binding to phosphotyrosine motifs of specific ligand receptors [4,5]. During activation, STATs can be specifically phosphorylated on both tyrosine and serine residues [4,6]. The phosphorylation of STAT3 at tyrosine 705 is important for nuclear translocation [6–8]. The phosphorylation of STAT3 at serine 727 located in a conserved Pro-X-Ser-Pro sequence has been shown to regulate STAT3-mediated transcriptional activation [4,6,9,10]. Once the activated STAT3 enters the nucleus, STAT3 binds to a *sis*-inducible element (SIE) of DNA [8]. After DNA binding, STAT3 proceeds to transactivate STAT-responsive genes such as Egr1 and JunB [1,11].

STATs have been reported to be activated by receptor tyrosine kinases (RTKs) [1,2,12]. Putative phosphotyrosine docking sites for STATs have been identified on EGF, PDGF, and insulin receptors (IR) [13–15]. However, the mechanism of STAT activation has been complicated by evidence suggesting that different RTKs potentially activate different STATs via distinct mechanisms. For instance, EGF and PDGF receptors appear to activate STAT1 and STAT3 via direct phosphorylation [16,17], whereas STAT3 activation by IGF-1 or PDGF receptors has been reported to depend on janus protein-tyrosine kinase (JAK) activation [15,18]. A conserved phosphorylation site for mitogen-activated protein kinase (MAPK) is present within the C-terminus of STAT3 and pS727-STAT3 is phosphorylated by extracellular signal-regulated protein kinases (ERK) in response to EGF [19–21]. In contrast, other reports indicate that the phosphorylation and activation of STAT3 are mediated through the phosphatidylinositol 3-kinase (PI3K)/mTOR signaling pathway [22,23]. On the other hand, independently of both MAPK and PI3K activation, PKC activation was required for pS727-STAT3 phosphorylation and transactivation in insulin-mediated signaling [10,24]. Thus, it has not been well established how the STAT3-mediated insulin signaling pathway works.

The structural components of caveolae are proteins belonging to the caveolin family. The three members of this family are caveolin-1, -2 and -3. Recent studies suggest that caveolins function as scaffolding proteins to interact with signaling molecules like G-proteins, RTKs, Src, eNOS, Ras, and ERK [25–27]. Thus, caveolin proteins take part in various cellular processes. The majority of the research on caveolin proteins has focused on the functions of caveolin-1 and -3. Caveolin-2, which is 38% identical and 58% similar to caveolin-1 is widely

* Corresponding author. Tel.: +82 55 751 5961; fax: +82 55 759 9363.
E-mail address: ybpak@nongae.gsnu.ac.kr (Y. Pak).

0167-4889/$ – see front matter © 2009 Elsevier B.V. All rights reserved.
doi:10.1016/j.bbamcr.2009.04.015

represented in various cell types [28,29] and has been noted for its structural role in caveolae formation without any significant implications in cell signaling [25–27,30]. Recent reports show that caveolin-2 can be tyrosine-phosphorylated on 19 by insulin [31,32] and on 19 and 27 by c-Src [32,33]. The tyrosine phosphorylation of caveolin-2 induces the binding of SH2-domain-containing proteins, c-Src, Nck, and Ras-GAP [32]. However, there have been no reports demonstrating that caveolin-2, per se, can modulate signaling in a manner similar to caveolin-1 and -3. Furthermore, involvement of caveolin-2 especially in the regulation of STAT3 signaling has not been shown.

We have recently reported that caveolin-2 regulates insulin-induced cell cycle and identified pY19-caveolin-2 as a regulator of insulin-stimulated mitogenesis in Hirc-B cells [31,34]. Hirc-B cells have been chosen as our model system to explore the regulatory role of caveolin-2 in insulin signaling due to their high expression of IRs [31,34,35] and having caveolin-2 as an endogenous caveolin isoform with no caveolin-1 gene expression [34]. In the studies, we demonstrated that induction of the caveolin-2 gene was up-regulated by insulin and caveolin-2 can associate with ERK. The caveolin-2 enhanced the G1 to S phase transition of cell cycle whereas caveolin-1 inhibits when cells were expressed with recombinant caveolin-1. Moreover, we showed that insulin-triggered phosphorylation of caveolin-2 at tyrosine 19 and the pY19-caveolin-2 was essential for interaction of caveolin-2 with phospho-ERK and their nuclear co-localization. And their interaction and nuclear localization in response to insulin were inhibited by U0126. Thus, our findings raised the possibility that caveolin-2 may act as a regulator for STAT3 activation and its regulation of cellular functions in insulin signaling pathway.

The present study was conducted to explore that tyrosine phosphorylation of caveolin-2 plays a role for STAT3-mediated transcriptional activation. Here, we provide evidence that phosphorylation of caveolin-2 at tyrosines 19 and 27 is required for activation, nuclear translocation, and transcriptional activity of STAT3 in response to insulin.

2. Materials and methods

2.1. Cell culture and treatment

Human insulin receptor-overexpressed rat 1 fibroblast (Hirc-B) cells were grown in DMEM containing 5 mM D-glucose supplemented with 10% (v/v) fetal bovine serum (FBS) (Cambrex Bio Science), 100 nM methotrexate (Sigma-Aldrich), and 0.5% gentamycin (Gibco) in a 5% CO2 incubator at 37 °C [31,34,35]. Cells were serum-starved in serum-free DMEM containing 0.2% BSA for 4 or 18 h as indicated and treated with or without 100 nM insulin (Human insulin, Novo Nordisk) for various period time as indicated.

2.2. Immunoblotting

For protein extraction, cells were washed twice with ice-cold phosphate-buffered saline (PBS) and lysed with RIPA buffer (50 mM HEPES, 150 mM NaCl, 100 mM Tris–HCl (pH 8.0), 0.25% deoxycholic acid, 0.1% SDS, 5 mM EDTA, 10 mM NaF, 5 mM DTT, 1 mM phenylmethylsulfonyl fluoride (PMSF), 1 mM sodium ortho-vanadate, 20 μM leupeptin, and 100 μM aprotinin). The lysate was put on ice for 30 min and microcentrifuged at 12,000 rpm for 20 min at 4 °C. Aliquots from the clear supernatant were taken for protein quantification as determined by the Bradford assay (Bio Rad). Equal amounts of samples (50 μg) were separated on 15% (w/v) SDS-polyacrylamide gels and transferred to polyvinylidene difluoride (PVDF) membrane (Millipore). Transfers were blocked overnight at 4 °C with 5% (v/v) nonfat dry milk in TBS, 0.1% (v/v) Tween 20, and then incubated for 2 h at room temperature (RT) in the primary antibody. The primary antibodies used were as follows: caveolin-2 mouse IgG1 (Clone 65, BD 610685; diluted 1/250), caveolin-1 mouse IgG1 (Clone 2297, BD 610407; diluted 1/1000), ERK (BD 610031; 1/2500), and STAT3 (BD 610190; 1/2500) antibodies from BD Transduction Laboratories; pY19-caveolin-2 (ab3417; 1/500) antibody from Abcam; F-actin (sc-1616; 1/200) antibody from Santa Cruz Biotechnology; phospho-ERK (Thr202 and Tyr204) (#9101; 1/1000), pS727-STAT3 (#9136; 1/1000), and pY705-STAT3 (#9135; 1/1000) antibodies from Cell Signaling; M2 FLAG (F1804; 1/1000) antibody from Sigma. The membranes were washed with TBS, 0.1% (v/v) Tween 20 and incubated for 1 h at RT in horseradish peroxidase-conjugated anti-rabbit (#W4011; 1/15000) or anti-mouse (#W4021; 1/15000) secondary antibodies (Promega) in 5% (v/v) nonfat dry milk in TBS, 0.1% (v/v) Tween 20. The immunoblots were developed using the ECL detection reagent (RPN2106, Amersham Biosciences).

2.3. Immunoprecipitation

Serum-starved cells were incubated with or without 100 nM insulin for 10 min, washed with ice-cold PBS and lysed in buffer A containing 1% Triton X-100, 150 mM NaCl, 10 mM Tris–HCl (pH 7.4), 1 mM EDTA, 1 mM EGTA (pH 8.0), 0.2 mM sodium ortho-vanadate, 0.2 mM PMSF, 0.5% Nonidet P-40 (Igepal CA-630, octylphenoxylpolyethoxylethanol, 198596; ICN Biomedicals), and 60 mM n-octylglucoside (OG, 494460, Calbiochem) [31]. The cell lysates were centrifuged at 12,000 rpm for 20 min at 4 °C and the supernatants were subjected to immunoprecipitation with either anti-caveolin-2, anti-STAT3, or anti-FLAG antibodies. Lysates were rotated overnight at 4 °C, then 30 μl of protein G plus Agarose (Calbiochem) was added and the mixture was rotated for 4 h at 4 °C. The immunocomplexes were collected by centrifugation at 12,000 rpm for 10 min 4 °C and washed three times with ice-cold buffer B (1% Triton X-100, 150 mM NaCl, 10 mM Tris–HCl (pH 7.4), 1 mM EDTA, 1 mM EGTA (pH 8.0), 0.2 mM sodium ortho-vanadate, 0.2 mM PMSF, 0.5% Nonidet P-40). After the final wash the pellet was resuspended in 30 μl of 2× SDS-PAGE sample buffer. Immunoprecipitated samples were then resolved, separated by SDS-PAGE, and subjected to immunoblot analyses using the specific antibodies against proteins of interest.

2.4. Silencing of the caveolin-2

The small interfering RNAs (siRNAs) were designed to target the following sequences: scramble control; 5′-GGAAAGACUGUUC-CAAAAA-3′, caveolin-2 siRNA duplexes; sense (GUAAAGACCUGC-CUAAUGGUU) and antisense (5′-PCCAUUAGGCAGGUCUUUACUU). The siRNA duplexes were synthesized and purified by Dharmacon Research, Inc. Briefly, transfection of siRNA duplexes was carried out using DhamaFECT Transfection Reagents (Dharmacon) for 48 h. The transfected cells were serum-starved for 4 h and followed by stimulation with or without 100 nM insulin for 10 min. Cells were then subjected to immunoblot analysis and processed for immunofluorescence microscopy as described below.

2.5. Plasmids

A full-length caveolin-2 cDNA (NM_131914) was subcloned into pcDNA3 vector (Invitrogen) [31]. Constructs encoding wild type (WT) caveolin-2 and point mutants including Y19A, Y27A, and Y19A/Y27A were generated by PCR mutagenesis using mutated oligonucleotides. FLAG-tagged caveolin-2 variants were cloned via PCR-based gateway cloning method as described previously [36]. Briefly, the caveolin-2 variants were amplified, cloned into pDONR207 vectors, and converted into pDS_EGFP-XB (a gift from Dr. Tobias Meyer, Stanford University) or self-made pDS_FLAG-XB vectors. The pDS_FLAG-XB vectors were generated by exchanging EGFP sequences of pDS_EGFP-XB vectors with FLAG sequences using an EZ change site-directed mutagenesis kit (Enzynomics, Daejeon, Korea). The plasmids were transiently transfected into cells using the Lipofectamine LTX transfection reagent (Invitrogen) as per the manufacturer's

instructions. Thirty-six hours post-transfection, cells were scraped into boiling sample buffer. Recombinant expression was confirmed by immunoblotting.

2.6. Fluorescence microscopy and quantitative detection of fluorescence staining

Effects of insulin and caveolin-2 variants on cellular translocation of caveolin-2, pY705-STAT3, and phospho-ERK were investigated by immunostaining cells. Briefly, transfected cells were serum-starved for 4 h in DMEM containing 0.2% BSA. Cells were then incubated with or without 100 nM insulin for 10 min, washed twice with ice-cold PBS, and fixed with 3.7% paraformaldehyde in PBS for 20 min at RT. The fixed cells were rinsed with PBS and incubated with 0.1% Triton X-100 in PBS for 30 min. Permeabilized cells were rinsed with PBS, incubated with 1% BSA in PBS for 30 min and then with anti-FLAG, anti-pY705-STAT3, and anti-phospho-ERK antibodies in 1% BSA in PBS for 2 h at RT. After washing three times with PBS, the primary antibodies were detected with either Alexa Fluor®488-conjugated anti-mouse (1/250 dilution) (Invitrogen) or TRITC-conjugated anti-rabbit (1/100 dilution) (Sigma) IgG antibodies for FLAG, pY705-STAT3 and phospho-ERK as indicated. Nuclei were fluorescently labeled with 4′, 6-diamidino-2-phenylinodole (DAPI) (D8417: Sigma) for 15 min at RT. The coverslips were then washed and mounted on glass slides. Fluorescent images were obtained using appropriate filters on an Olympus BX51 microscope and imaged with an Olympus DP-71 digital camera with an image processing system equipped with Image-ProPlus 6.1 (MediaCybernetics). Neither labeling in the absence of the primary antibody nor cross-reactivity between secondary and primary antibodies was observed. Fluorescence staining was quantified by image analysis performed using ImageJ software (National Institutes of Health) as previously described [31]. The DAPI staining mask was used to define the nuclear region of interest (ROI). Briefly, using the Image Calculator from ImageJ, the DAPI mask was subtracted from the merge mask to create a staining mask defining the cytoplasmic ROI. Nuclear and cytoplasmic staining intensities were compared to give the nuclear:cytoplasmic ratio. Averages and standard errors were computed over 5 images per condition for a minimum of 200 cells per condition.

2.7. DNA binding assay

Whole cell lysates were prepared using lysis buffer (1% Triton X-100, 50 mM NaCl, 10 mM Tris (pH 7.5), 1 mM EDTA, 0.2 mM sodium orthovanadate, 0.2 mM PMSF, and 0.5% Nonidet P-40). The whole cell lysates were incubated with 10 μg of SIE-oligonucleotide agarose beads (Santa Cruz) for overnight at 4 °C. After incubation, the beads were washed with binding buffer (10 mM Tris (pH 7.5), 50 mM NaCl, 1 mM DTT, 1 mM EDTA, 5% glycerol, and 1 μg/ml poly dI-dC), and then proteins were eluted from beads with elution buffer (same as the binding buffer but containing 150 mM NaCl). The SIE bead-precipitated proteins were separated by SDS-PAGE and then transferred to PVDF membranes for immunoblotting with anti-pS727-STAT3 and anti-STAT3 antibodies.

2.8. Reverse transcription-PCR

Total RNA was extracted with TRIzol reagent (SolGent Co., Ltd.) according to the manufacturer's instructions. cDNA was generated using reverse transcription kit (Accupower RT PreMix, Bioneer). The cDNA was used as the template for the subsequent PCR amplification. PCR primers were for glyceraldehyde-3-phosphate dehydrogenase (GAPDH): 5′-ACCACCATGGAGAAGGCTGG-3′ and 5′-CTCAGTGTAGCCCAGGATGCC-3′; JunB: 5′-ACTCTTACG-CAGCGGCAGG-3′ and 5′-AGTAACTGCTGAGGTTGGTGTAGACC-3′; Erg1: 5′-GACAGCAGTCCCATTTACTCAGCT-3′ and 5′-TGTCACAGG-CAAAAGGCTTCTC-3′. PCR was performed using AccuPower PCR PreMix (Bioneer) kit. The PCR fragments were separated by running on 1% agarose gels.

2.9. Luciferase reporter assay

STAT3 TransLucent Reporter Vector (STAT3-Luc) to monitor transcription factor binding activity of STAT3 was purchased from

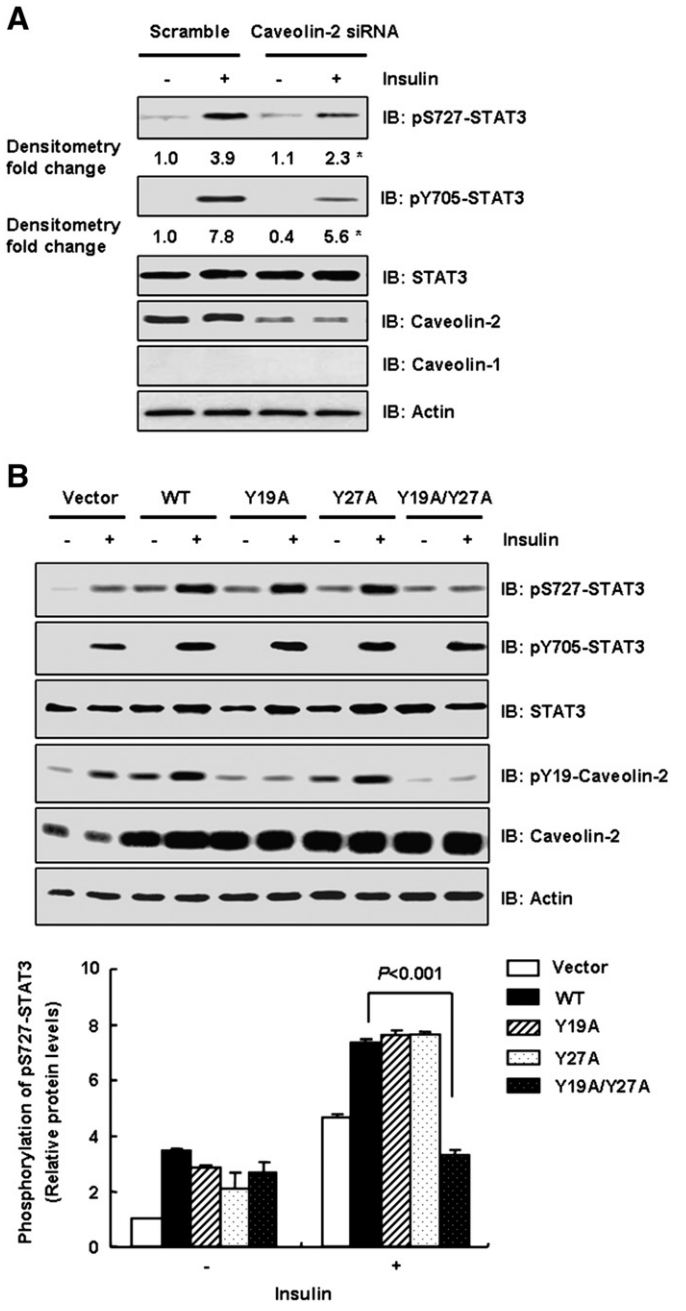

Fig. 1. Phosphorylation of STAT3 is decreased by caveolin-2 siRNA and tyrosine mutants. (A) Hirc-B cells were transfected with scramble or caveolin-2 siRNAs for 48 h. The cells were treated with or without insulin (100 nM) for 10 min. Whole cell lysates (WCL) were subjected to immunoblotting using antibodies specific for pS727-STAT3, pY705-STAT3, STAT3, caveolin-2, caveolin-1 and actin. Numerical data represent the mean ± S.E. of results that were repeated three times each with similar results; * comparison with their scramble controls, $P<0.05$. (B) Cells were transfected with pcDNA3 vector, wild type (WT) caveolin-2, Y19A-caveolin-2, Y27A-caveolin-2, or Y19A/Y27A-caveolin-2. Thirty-six hours post-transfection, the cells were treated with or without insulin (100 nM) for 10 min. WCL were subjected to immunoblot analysis with anti-pS727-STAT3, anti-pY705-STAT3, anti-STAT3, anti-pY19-caveolin-2, anti-caveolin-2, and anti-actin antibodies as indicated. The results represent the mean ± S.E. of four independent experiments.

Panomics (Redwood City, CA). Cells were transiently transfected using the Lipofectamine LTX reagent (Invitrogen) with 0.5 μg of plasmid DNA (STAT3-Luc) along with the control pcDNA3, pcDNA3 + WT caveolin-2, pcDNA3 + Y19A-caveolin-2, pcDNA3 + Y27A-caveolin-2, or pcDNA3 + Y19A/Y27A-caveolin-2 in each well of 24-well plates. The Renilla reporter construct pRL-TK (Promega) was used to normalize the transfection efficiency. The cells were incubated for 24 h in DMEM containing 10% FBS and then serum-starved for 4 h in DMEM containing 2% BSA prior to stimulation with or without 100 nM insulin for 16 h. The cells were washed twice with ice-cold PBS and lysed in 100 μl/well of passive lysis buffer (Promega). Luciferase activity was measured using a dual-luciferase reporter assay system (Promega).

2.10. Densitometry analysis

Chemiluminescent images of immunoblots were analyzed by scanning densitometry using a Kodak Gel Logic 100 Imaging System (Eastman Kodak Co.). Multiple exposure of each blot was used to obtain gray-scale images of each chemiluminescent band. Bands were visualized on a UV transilluminator and photographed.

2.11. Statistical analysis

Data are expressed as mean ± S.E. An unpaired Student's *t* test was used to compare treatment groups with significance established at a level of $p<0.05$.

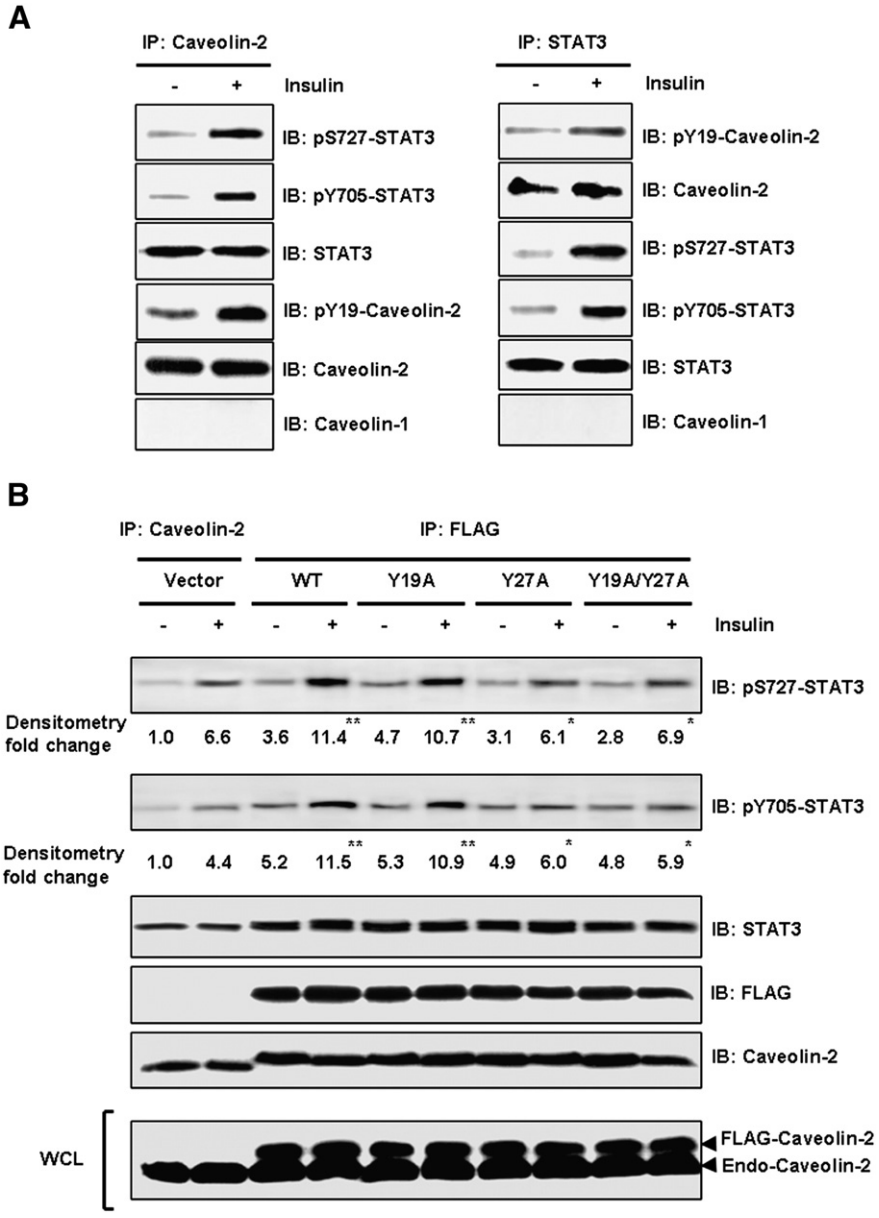

Fig. 2. Y27A-Caveolin-2 mutant decreases phosphorylation of STAT3 interacting with caveolin-2. (A) Hirc-B cells were serum-starved for 18 h and treated with or without insulin (100 nM) for 10 min. Equal amounts of WCL were immunoprecipitated with anti-caveolin-2 or anti-STAT3 antibodies and subjected to immunoblot analysis with anti-pS727-STAT3, anti-pY705-STAT3, anti-STAT3, anti-pY19-caveolin-2, anti-caveolin-2, and anti-caveolin-1 antibodies as indicated. A representative result from three independent immunoprecipitation experiments with anti-STAT3 or anti-caveolin-2 antibodies is shown. (B) Cells expressing pDS_FLAG-XB vector, FLAG-WT caveolin-2, FLAG-Y19A-caveolin-2, FLAG-Y27A-caveolin-2, or FLAG-Y19A/Y27A-caveolin-2 were treated with or without insulin (100 nM) for 10 min. WCL were immunoprecipitated with anti-caveolin-2 or anti-FLAG antibodies and subjected to immunoblot analysis with anti-pS727-STAT3, anti-pY705-STAT3, anti-STAT3, anti-FLAG, and anti-caveolin-2 antibodies as indicated. Numerical data represent the mean ± S.E. of results that were repeated three times each with similar results; * comparison with their respective vector controls, $P>0.05$. $^{**}P<0.001$.

3. Results

3.1. Phosphorylation of caveolin-2 at tyrosines 19 and 27 is important for pS727-STAT3 activation

To evaluate the role of caveolin-2 in STAT3 activation by insulin, cells were transfected with caveolin-2 specific siRNA. As shown in Fig. 1A, the caveolin-2 siRNAs effectively depleted caveolin-2 protein by over 80% of levels detected in the scramble control. Knockdown of caveolin-2 decreased phosphorylation of pS727- and pY705-STAT3 by 1.7 and 1.4 fold, respectively in response to insulin (Fig. 1A). As previously demonstrated [31,34], caveolin-1 was not detected and exhibited no changes by insulin and caveolin-2 siRNA in Hirc-B cells. Thus, the results show that caveolin-2 is required for insulin-stimulated phosphorylation of STAT3.

Caveolin-2 contains a consensus sequence (*QLFMADDSpY*) for phosphorylation by a tyrosine kinase at tyrosine 19 and a conserved SH2 domain-binding motif (*pYADP*) at tyrosine 27 [32,33]. To investigate how pY19- and pY27-caveolin-2 function in insulin-induced STAT3 signaling, we generated three tyrosine mutants of caveolin-2. As demonstrated in Fig. 1B, panel 4, Y19A- and Y19A/Y27A-caveolin-2 mutants are no longer phosphorylated at tyrosine 19. The caveolin-2 variants induced 2.1–3.4 fold increases in phosphorylation of pS727-STAT3 without insulin stimulation as compared to endogenous caveolin-2 (vector control) (Fig. 1B). Wild type (WT) caveolin-2 increased phosphorylation of pS727-STAT3 by 1.6 fold with insulin stimulation as compared to the basal increased level by endogenous caveolin-2. Y19A- or Y27A-Caveolin-2 mutants caused the same increases (1.6 fold) in the insulin-induced phosphorylation of pS727-STAT3 as observed by WT caveolin-2. Y19A/Y27A-Caveolin-2, however, decreased insulin-induced phosphorylation of pS727-STAT3 below the control endogenous caveolin-2 level. These results suggest that phosphorylation of caveolin-2 at tyrosines 19 as well as 27 is required for insulin-induced activation of pS727-STAT3. In contrast, insulin-stimulated phosphorylation of pY705-STAT3 exhibited no detectable changes by the caveolin-2 variants (Fig. 1B).

3.2. Caveolin-2 Y27A mutation decreases phosphorylation of caveolin-2-associated STAT3

As we investigated caveolin-2 interaction with STAT3, STAT3 association with caveolin-2 was observed in untreated cells and the amount of STAT3 interacting with caveolin-2 was not changed by insulin (Fig. 2A). Insulin triggered phosphorylation of pY19-caveolin-2 (Fig. 2A. left panel 4) as previously demonstrated [31] and increased the amount of pY19-caveolin-2 interacting with STAT3 (Fig. 2A, right panel 1). The amount of pS727- and pY705-STAT3 associated with caveolin-2 was increased by insulin. Caveolin-2 or

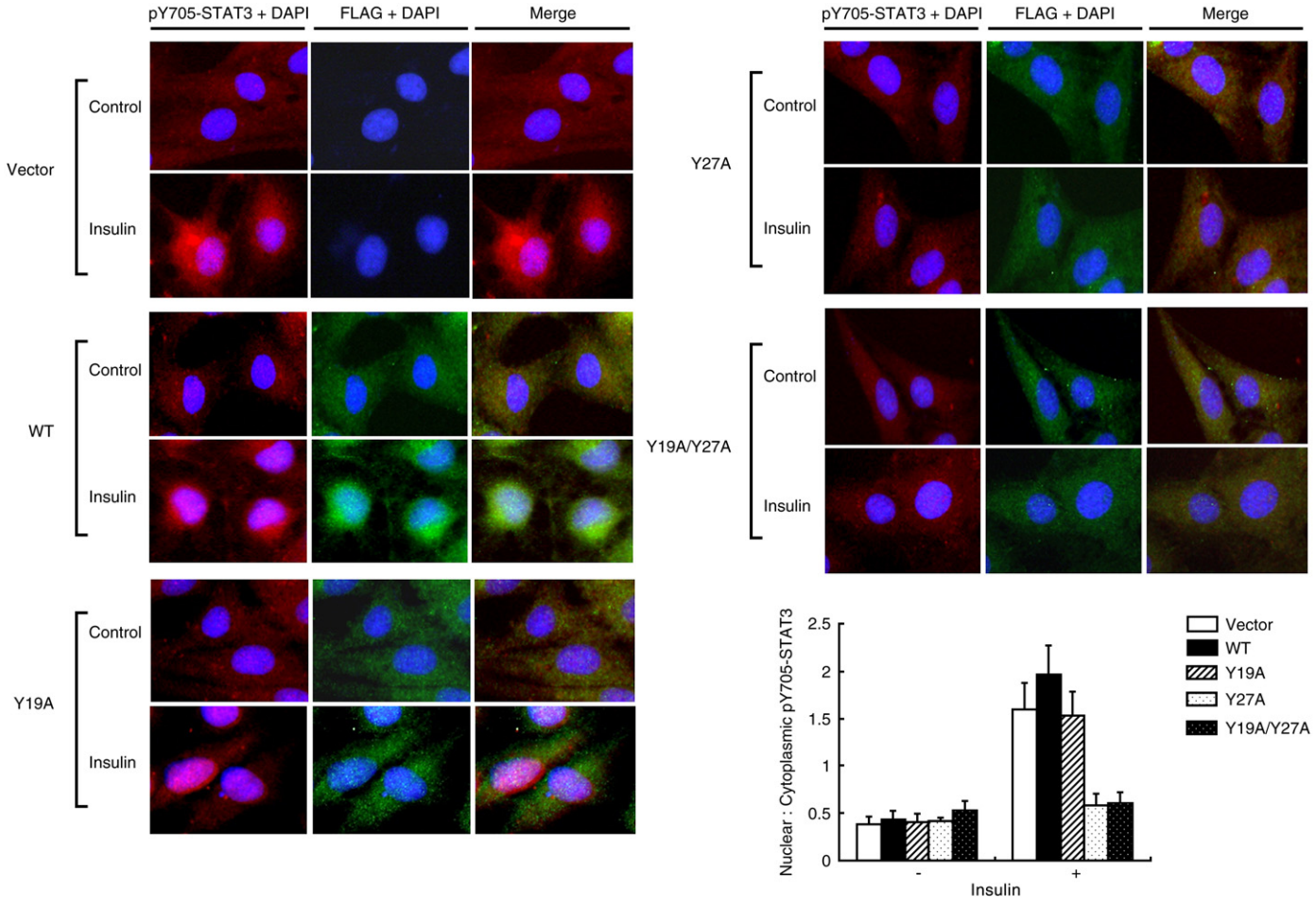

Fig. 3. Y27A-Caveolin-2 mutant prevents nuclear translocation of pY705-STAT3. Confluent cells grown on coverslips were transfected with pDS_FLAG-XB vector, FLAG-WT caveolin-2, FLAG-Y19A-caveolin-2, FLAG-Y27A-caveolin-2, or FLAG-Y19A/Y27A-caveolin-2. Thirty-six hours post-transfection, the cells were treated with or without insulin (100 nM) for 10 min. Cells were stained with anti-FLAG and anti-pY705-STAT3 antibodies followed by Alexa Fluor®488- or TRITC-conjugated antibodies, respectively. DNA was stained using DAPI to visualize the nucleus. pY705-STAT3 nuclear translocation was quantified by ImageJ. The results represent the mean ± S.E. from analysis of five separate field image of five independent experiments. A minimum of 200 cells per condition were counted. Red: pY705-STAT3, green: FLAG-caveolin-2 variants, merge: pY705-STAT3 + FLAG-caveolin-2 variants + DAPI.

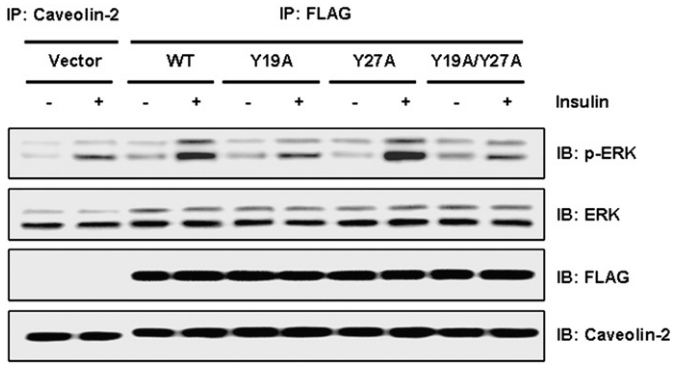

Fig. 4. Y19A-Caveolin-2 mutant attenuates phosphorylation of ERK interacting caveolin-2. Hirc-B cells expressing pDS_FLAG-XB vector, FLAG-WT caveolin-2, FLAG-Y19A-caveolin-2, FLAG-Y27A-caveolin-2, or FLAG-Y19A/Y27A-caveolin-2 were treated with or without insulin (100 nM) for 10 min. WCL were immunoprecipitated with anti-caveolin-2 or anti-FLAG antibodies and subjected to immunoblot analysis with anti-phospho-ERK, anti-ERK, anti-FLAG, and anti-caveolin-2 antibodies as indicated.

STAT3 interaction with caveolin-1 was not detected (Fig. 2A). When we explored the effect of caveolin-2 tyrosine mutation on the phosphorylation of pS727- and pY705-STAT3 using FLAG-tagged caveolin-2 variants, the caveolin-2 variants induced 2.8–4.7 and 4.8–5.3 fold increases in the phosphorylation of pS727- and pY705-STAT3, respectively without insulin stimulation (Fig. 2B). Insulin-induced phosphorylation of the caveolin-2-bound pS727- and pY705-STAT3 was 1.6–2.6 fold increased by WT and Y19A-caveolin-2 as compared to the increases by endogenous caveolin-2 (vector control). Caveolin-2 Y27A mutation, however, markedly decreased the phosphorylation of STAT3 close to the basal level by endogenous caveolin-2 in response to insulin. The reduction by Y27A-caveolin-2 was reconfirmed by expression of double mutant, Y19A/Y27A-caveolin-2 exhibiting almost the same degree of decrease as observed by Y27A-caveolin-2 (Fig. 2B). Together, these data suggest that there is a sub-pool of STAT3 that becomes phosphorylated while bound to caveolin-2, and that this activation requires phosphorylation of caveolin-2 on tyrosine 27 in response to insulin.

3.3. Caveolin-2 Y27A mutation impairs nuclear translocation of pY705-STAT3

Transcriptional activation of STAT3 is characterized by nuclear translocation of pY705-STAT3 [1]. To study the functional significance of two tyrosine-phosphorylated forms of caveolin-2 on the translocation of pY705-STAT3, we examined effect of FLAG-tagged caveolin-2

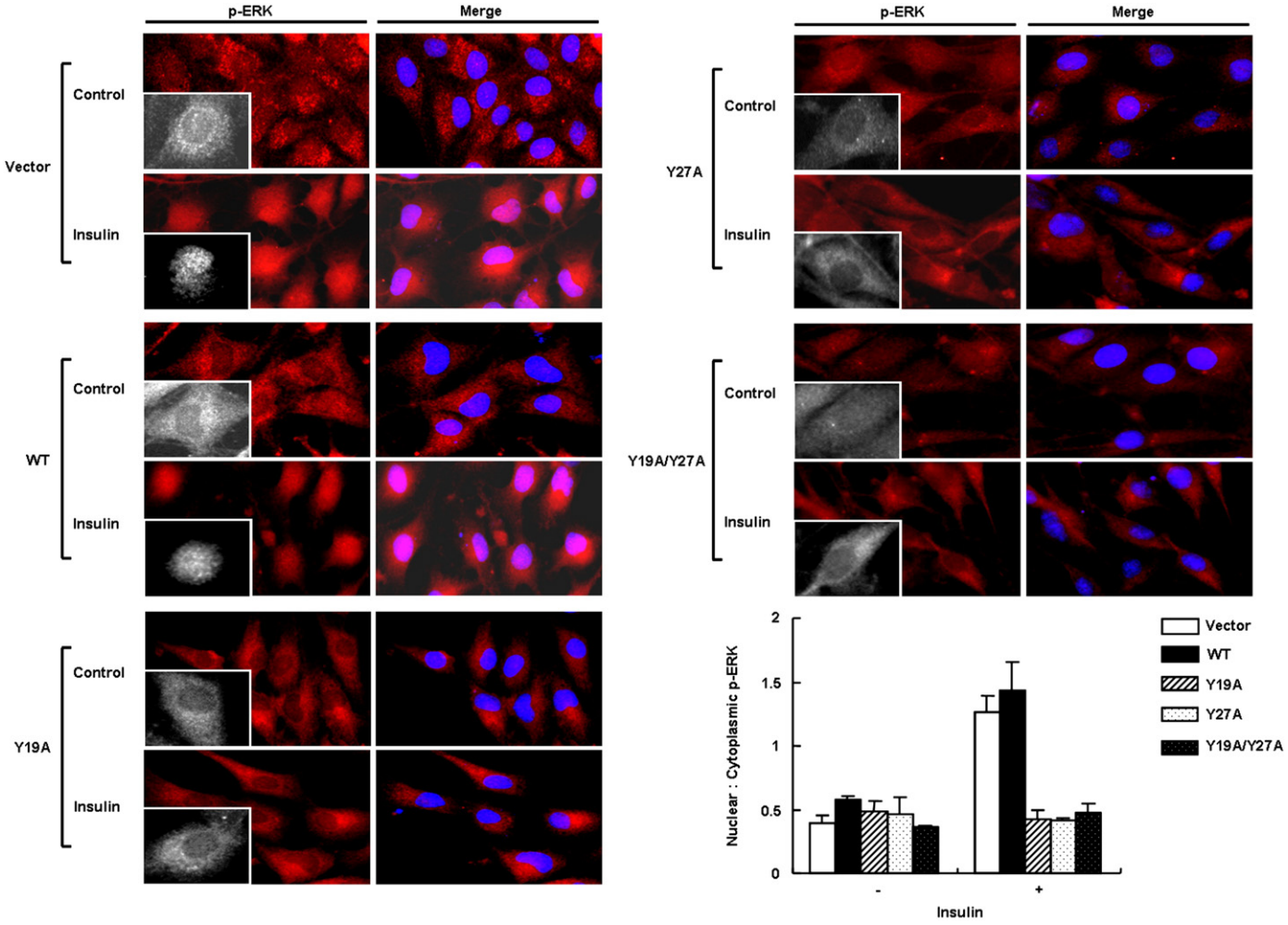

Fig. 5. Y19A-Caveolin-2 mutant impedes nuclear localization of phospho-ERK. Confluent cells grown on coverslips were transfected with pDS_FLAG-XB vector, FLAG-WT caveolin-2, FLAG-Y19A-caveolin-2, FLAG-Y27A-caveolin-2, or FLAG-Y19A/Y27A-caveolin-2. Thirty-six hours post-transfection, the cells were treated with or without insulin (100 nM) for 10 min. Cells were stained with anti-phospho-ERK antibody followed by TRITC-conjugated antibody. DNA was stained using DAPI to visualize the nucleus. Phospho-ERK nuclear translocation was quantified by ImageJ. The results represent the mean ± S.E. from analysis of five separate field images of three independent experiments. A minimum of 200 cells per condition were counted. Red: phospho-ERK, merge: phospho-ERK + DAPI.

tyrosine mutants on immunofluorescence localization of pY705-STAT3 in response to insulin. Insulin triggered nuclear translocation of pY705-STAT3 in vector control. While WT and Y19A-caveolin-2 promoted translocation of pY705-STAT3 to the nucleus, Y27A- and Y19A/Y27A-caveolin-2 blocked the nuclear translocation in response to insulin (Fig. 3). Consistent with the results, quantitative data showed decreases in nuclear:cytoplasmic ratios of pY705-STAT3 staining by Y27A- and Y19A/Y27A-caveolin-2 mutants in response to insulin. When we examined nuclear translocation of the caveolin-2 variants, insulin re-localized WT caveolin-2 to the nucleus. However, Y19A-, Y27A-, and Y19A/Y27A-caveolin-2 remained in the cytoplasm suggesting both pY19- and pY27-caveolin-2 are required for nuclear localization of caveolin-2 in response to insulin. Thus, our data show that phosphorylation of caveolin-2 at tyrosine 27 influences insulin-induced nuclear translocation of pY705-STAT3.

3.4. pY19-Caveolin-2 regulates nuclear translocation of phospho-ERK

Since pY27-caveolin-2 influenced insulin-induced phosphorylation of STAT3 interacting with caveolin-2 as demonstrated in Fig. 2, we next investigated if pY27-caveolin-2 affects phosphorylation of ERK, which is known to activate pS727-STAT3 [19–21], using FLAG-tagged caveolin-2 variants (Fig. 4). Caveolin-2 variants increased phosphorylation of ERK associated with caveolin-2 (3.0–3.8 fold) without insulin stimulation (Fig. 4). The phosphorylation of ERK was 2.0–2.4 fold increased by WT and Y27A-caveolin-2 as compared to the increase by endogenous caveolin-2 (vector control) in response to insulin. In our previous study, we showed that phosphorylation of ERK associated with caveolin-2 is increased by pY19-caveolin-2 [31]. Consistent with the finding, Y19A-caveolin-2 mutation decreased the phosphorylation of ERK and the reduction was reconfirmed by Y19A/Y27A-caveolin-2 double mutant (Fig. 4). Thus, our present data reconfirm and reveal that pY19-caveolin-2, but not pY27-caveolin-2, is essential for insulin-induced phosphorylation of ERK interacting with caveolin-2. Together, the data demonstrated in Fig. 2B point out that pY27-caveolin-2, but not pY19-caveolin-2, is required for phosphorylation of STAT3 interacting with caveolin-2 in response to insulin.

In addition to insulin-triggered interaction between pY19-caveolin-2 and phospho-ERK, insulin re-localized the pY19-caveolin-2 and phospho-ERK to the nucleus [31]. To examine whether the nuclear localization of phospho-ERK is affected by phosphorylation of caveolin-2 on tyrosines 19 and 27, the effect of caveolin-2 tyrosine mutants on immunofluorescence localization of phospho-ERK was investigated. In untreated cells, phospho-ERK was localized at the cytoplasm (Fig. 5). Insulin triggered translocation of phospho-ERK to the nucleus in vector control and WT caveolin-2-transfected cells. The localization of phospho-ERK, however, was retarded by Y19A- and Y27A-caveolin-2 mutation (Fig. 5). The retardation of phospho-ERK was reconfirmed by Y19A/Y27A-caveolin-2 double mutation. Consistent with the results, quantitative data showed decreases in nuclear:cytoplasmic ratios of phospho-ERK staining by Y19A-, Y27A- and Y19A/Y27A-caveolin-2 mutants in response to insulin. Thus, the data show that pY19- and pY27-caveolin-2 are required for the insulin-induced nuclear localization of ERK.

3.5. pY19-Caveolin-2 enhances DNA binding activity of pS727-STAT3 and STAT3-induced immediate early gene transcription

Although nuclear translocation of phospho-ERK was impaired by Y19A-caveolin-2, STAT3 became phosphorylated and pY705-STAT3 re-localized to the nucleus in response to insulin (Figs. 2–5). It has been reported that ERK phosphorylates pS727-STAT3 [19–21], which, in turn, promotes STAT3-mediated transcriptional activation [4,6,9,10]. Thus, we postulated that the retardation in nuclear translocation of phospho-ERK by Y19A-caveolin-2 leads to impairment of pS727-STAT3 function in the nucleus. Accordingly, we investigated the effect of pY19-caveolin-2 in insulin-induced STAT3 regulation in the nucleus. First, to examine insulin-induced DNA binding activity of STAT3, a DNA binding assay using SIE oligo-agarose beads was performed. As shown in Fig. 6A, insulin stimulated DNA binding of STAT3, which was not observed in the absence of insulin stimulation (vector control). When the blot was stripped and re-probed with anti-phospho-STAT3 antibodies, pS727-STAT3, but not pY705-STAT3 (data not shown), was detected. WT caveolin-2 overexpression increased DNA binding of STAT3 but the binding activity was not changed by insulin stimulation. Further, the STAT3 DNA binding was not affected by Y19A- and Y19A/Y27A-caveolin-2 mutants (Fig. 6A, panel 2). When DNA binding of pS727-STAT3 was examined, the caveolin-2 variants induced 4.7–6.3 fold increases without insulin stimulation (Fig. 6A, panel 1). DNA binding of pS727-STAT3 in response to insulin was 1.5 fold increased by WT caveolin-2 as compared to the increase by endogenous caveolin-2 (vector control). Y19A- and

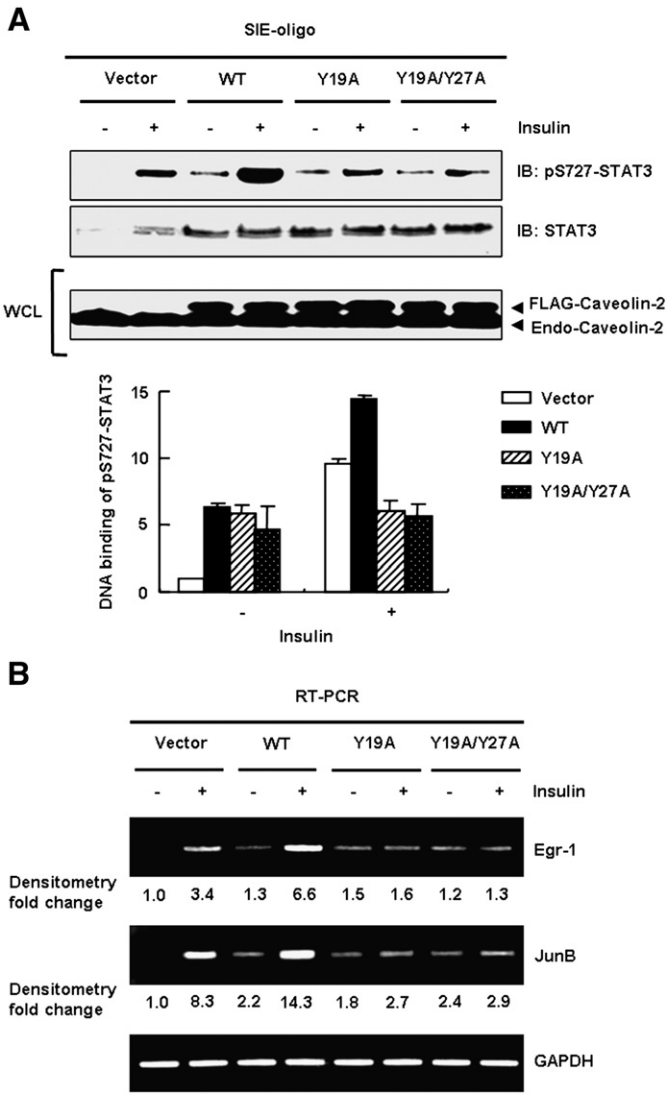

Fig. 6. Y19A-Caveolin-2 mutant decreases DNA binding of pS727-STAT3 and STAT3-mediated immediate early gene induction. (A) Hirc-B cells expressing pDS_FLAG-XB vector, FLAG-WT caveolin-2, FLAG-Y19A-caveolin-2, or FLAG-Y19A/Y27A-caveolin-2 were treated with or without insulin (100 nM) for 10 min. The DNA binding activity of the cell lysates were detected as described above. The results represent the mean ± S.E. of three independent experiments. (B) Cells were transfected with pcDNA vector, WT caveolin-2, Y19A-caveolin-2, or Y19A/Y27A-caveolin-2. Thirty-six hours post-transfection, the cells were treated with or without insulin (100 nM) for 60 min. Egr-1 and JunB mRNA levels were analyzed by the RT-PCR. Numerical data represent the mean ± S.E. of results that were repeated three times each with similar results. GAPDH was co-amplified as the internal control.

Y19A/Y27A-caveolin-2, however, decreased the DNA binding below the endogenous caveolin-2 level. Thus, these data reveal that pY19-caveolin-2 regulates insulin-induced DNA binding of pS727-STAT3 in the nucleus.

Next, to investigate a regulatory role of pY19-caveolin-2 in STAT3-induced early gene transcription, the immediate early gene induction in response to insulin was examined by RT-PCR analysis. As shown in Fig. 6B, insulin-elicited Egr-1 and JunB transcription was increased by WT caveolin-2. The Egr-1 and JunB transcription, however, was decreased to the control levels by Y19A- and Y19A/Y27A-caveolin-2 mutants. Taken together, our findings indicate that pY19-caveolin-2 regulates insulin-induced DNA binding activity of pS727-STAT3 and STAT3-targeted immediate early gene induction in the nucleus.

3.6. Phosphotyrosine-caveolin-2 regulates transcriptional activation of STAT3

To further evaluate whether caveolin-2 controls the transcriptional activation of STAT3 by insulin, we performed a reporter gene assay using a luciferase reporter construct containing STAT3-binding sites. Insulin enhanced STAT3-mediated transcriptional activation by a 1.9 fold (Fig. 7A). However, down-regulation of caveolin-2 caused 63% suppression in the insulin-induced STAT3-mediated transcriptional activity. When the effect of tyrosine phosphorylation of caveolin-2 was examined, STAT3-mediated transcriptional activity was 1.3–1.7 fold up-regulated by caveolin-2 variants as compared to endogenous caveolin-2 (vector control) without insulin stimulation (Fig. 7B). WT

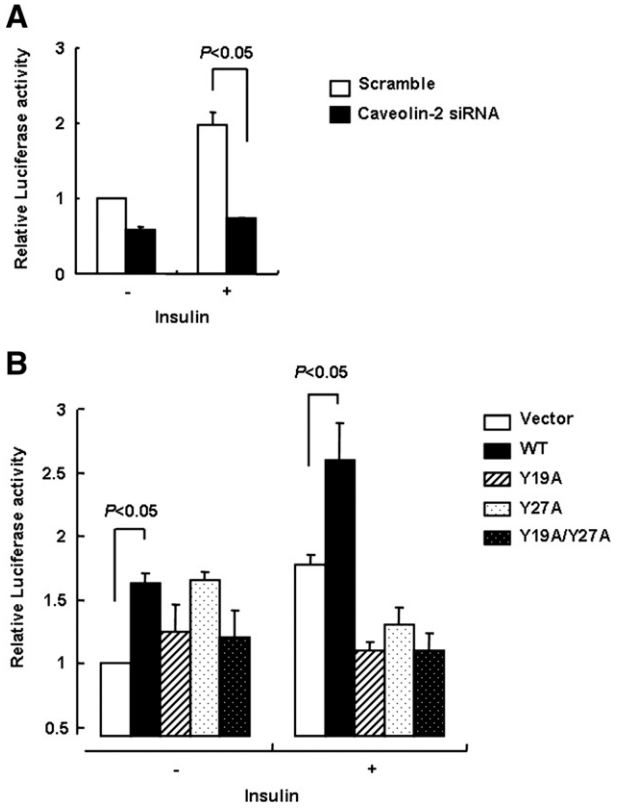

Fig. 7. Caveolin-2 siRNA and caveolin-2 tyrosine mutants attenuate transcriptional activation of STAT3. (A) Hirc-B cells were co-transfected with scramble or caveolin-2 siRNAs and STAT3-Luc with pRL-TK vectors for 48 h. The cells were treated with or without insulin (100 nM) for 16 h. Luciferase activity was measured with the dual-luciferase assay system and data were presented as the mean ± S.E. of three independent experiments performed. (B) Cells were co-transfected with pcDNA vector, WT caveolin-2, Y19A-caveolin-2, Y27A-caveolin-2, or Y19A/Y27A-caveolin-2 and STAT3-Luc with pRL-TK vectors for 48 h. The cells were treated with or without insulin (100 nM) for 16 h. The results represent the mean ± S.E. of three independent experiments.

Caveolin-2 increased the STAT3-mediated transcriptional activation by 1.5 fold with insulin stimulation as compared to the basal increased level by endogenous caveolin-2. Y19A-, Y27A- or Y19A/Y27A-caveolin-2, however, completely inhibited the transcriptional activation below the basal level by endogenous caveolin-2. Thus, these data demonstrate that phosphorylation of caveolin-2 at tyrosines 19 and 27 is required for the transcriptional activation of STAT3 in response to insulin.

4. Discussion

Our first investigation for the functional role of insulin-induced tyrosine phosphorylation of caveolin-2 has revealed that phosphorylation of pY19-caveolin-2 is required for ERK-mediated mitogenic regulation of insulin signaling [31]. The present results identify that pY27- and pY19-caveolin-2 regulate STAT3 activation. To define the regulatory mechanism by pY27- and pY19-caveolin-2 involved in STAT3 activation in insulin signaling, we investigated effect of caveolin-2 tyrosine variant mutants. Mutation of either of these two tyrosines to alanine does not influence insulin-induced activation of pY727- and pY705-STAT3, but double mutation of tyrosines 19 and 27 completely inhibited the phosphorylation of pS727-STAT3. Thus, the present results demonstrate that phosphorylation of caveolin-2 at tyrosines 19 and 27 is required for pS727-STAT3 activation.

One of the well known functions of tyrosine phosphorylation is to confer docking sites for SH2 domain-containing proteins. STATs have a SH2 domain near the C-terminus [4,5]. Caveolin-2 contains a conserved motif at tyrosine 27 for recognition by SH2 domain-containing proteins [32,33]. To our knowledge, our data show the first demonstration that caveolin-2 interacts with STAT3. Of interest, insulin did not affect the total amount of STAT3 that is associated with caveolin-2. However, insulin increased phosphorylation of STAT3 interacting with caveolin-2. The phosphorylation of pS727- and pY705-STAT3 was markedly decreased by Y27A-caveolin-2 mutation. In parallel, insulin-induced nuclear translocation of pY705-STAT3 was blocked by Y27A-caveolin-2. These results collectively reveal that pY27-caveolin-2 is critical not only for phosphorylation of STAT3 interacting with caveolin-2 but also nuclear translocation of pY705-STAT3 in response to insulin.

In contrast to the results by Y27A-caveolin-2, Y19A-caveolin-2 mutation exhibited no effect on the phosphorylation of STAT3 and nuclear localization of pY705-STAT3. We have previously shown that insulin promotes nuclear translocation of pY19-caveolin-2 and phospho-ERK and demonstrated that their nuclear translocation is inhibited by U0126 [31]. The present data demonstrate that Y19A-caveolin-2 remains in cytoplasm in response to insulin and that the Y19A-caveolin-2 attenuates translocation of phospho-ERK to the nucleus. Since pS727-STAT3 is known to be phosphorylated by ERK [19–21], we investigated whether the nuclear localized STAT3 carries on transcriptional activation in the nucleus where pY19-caveolin-2 and phospho-ERK are absent. Mutation of caveolin-2 at tyrosine 19 markedly decreased insulin-induced DNA binding of pS727-STAT3 in the nucleus. Moreover, insulin-induced STAT3-responsive induction of Egr-1 and JunB genes was also dependent on phosphorylation of pY19-caveolin-2. Thus, our data suggest that the impairment of nuclear translocation of phospho-ERK by Y19A-caveolin-2 mutation leads to the attenuation on the ERK-mediated phosphorylation of pS727-STAT3 required for DNA binding and early gene transcription of STAT3 in the nucleus. Finally, our results from the STAT3-specific luciferase reporter assay demonstrate that phosphorylation of caveolin-2 at tyrosines 19 and 27 is required for insulin-stimulated transcriptional activation of STAT3. Collectively, the present data support that insulin-induced STAT3-dependent transcription is regulated by phosphorylation of caveolin-2 at tyrosines 19 as well as 27.

In summary, the present study suggests that pY27-caveolin-2 re-localizes pY705-STAT3 to the nucleus in response to insulin. pY19-Caveolin-2-regulated ERK activates pS727-STAT3 in the nucleus,

thereby promoting pY19-caveolin-2-dependent DNA binding of pS727-STAT3 and, in turn, STAT3-mediated transcriptional activation. Thus, the phosphotyrosine-caveolin-2 acts as an important component in STAT3 transcriptional activation regulated by cross-talk among caveolin-2, ERK and STAT3 in insulin signaling. STAT3 is constitutively activated in many human cancers [37,38]. Oncogenic STAT3, which is not dependent on phosphorylation by JAK, cannot be down-regulated by SOCS1 [39]. Caveolin-2 is widely presented in both normal and tumor cells [29]. Therefore, the inhibition of tyrosine phosphorylation of caveolin-2 could be a novel molecular target for the regulation of oncogenic STAT3 in various cancers.

Acknowledgements

HK and KJ were supported by a scholarship from the BK21 Program, the Ministry of Education, Science and Technology, Korea.

References

[1] J.E. Darnell Jr, STATs and gene regulation, Science 277 (1997) 1630–1635.
[2] D.E. Levy, J.E. Darnell Jr, Stats: transcriptional control and biological impact, Nat. Rev. Mol. Cell Biol. 3 (2002) 651–662.
[3] J. Bromberg, J.E. Darnell Jr, The role of STATs in transcriptional control and their impact on cellular function, Oncogene 19 (2000) 2468–2473.
[4] J.F. Bromberg, C.M. Horvath, D. Besser, W.W. Lathem, J.E. Darnell Jr, Stat3 activation is required for cellular transformation by v-src, Mol. Cell. Biol. 18 (1998) 2553–2558.
[5] A.C. Greenlund, M.O. Morales, B.L. Viviano, H. Yan, J. Krolewski, R.D. Schreiber, Stat recruitment by tyrosine-phosphorylated cytokine receptors: an ordered reversible affinity-driven process, Immunity 2 (1995) 677–687.
[6] T. Decker, P. Kovarik, Serine phosphorylation of STATs, Oncogene 19 (2000) 2628–2637.
[7] X. Chen, U. Vinkemeier, Y. Zhao, D. Jeruzalmi, J.E. Darnell Jr, J. Kuriyan, Crystal structure of a tyrosine-phosphorylated STAT-1 dimer bound to DNA, Cell 93 (1998) 827–839.
[8] Z. Zhong, Z. Wen, J.E. Darnell Jr, Stat3: a STAT family member activated by tyrosine phosphorylation in response to epidermal growth factor and interleukin-6, Science 264 (1994) 95–98.
[9] K. Abe, M. Hirai, K. Mizuno, N. Higashi, T. Sekimoto, T. Miki, T. Hirano, K. Nakajima, The YXXQ motif in gp130 is crucial for STAT3 phosphorylation at Ser727 through an H7-sensitive kinase pathway, Oncogene 20 (2001) 3464–3474.
[10] M. Gartsbein, A. Alt, K. Hashimoto, K. Nakajima, T. Kuroki, T. Tennenbaum, The role of protein kinase C delta activation and STAT3 Ser727 phosphorylation in insulin-induced keratinocyte proliferation, J. Cell. Sci. 119 (2006) 470–481.
[11] R. Wang, P. Cherukuri, J. Luo, Activation of Stat3 sequence-specific DNA binding and transcription by p300/CBP mediated acetylation, J. Biol. Chem. 280 (2005) 11528–11534.
[12] J.S. Rawlings, K.M. Rosler, D.A. Harrison, The JAK/STAT signaling pathway, J. Cell. Sci. 117 (2004) 1281–1283.
[13] J. Chen, H.B. Sadowski, R.A. Kohanski, L.H. Wang, Stat5 is a physiological substrate of the insulin receptor, Proc. Natl. Acad. Sci. U. S. A. 94 (1997) 2295–2300.
[14] P.J. Coffer, W. Kruijer, EGF receptor deletions define a region specifically mediating STAT transcription factor activation, Biochem. Biophys. Res. Comm. 210 (1995) 74–81.
[15] S. Valgeirsdóttir, K. Paukku, O. Silvennoinen, C.H. Heldin, L. Claesson-Welsh, Activation of Stat5 by platelet-derived growth factor (PDGF) is dependent on phosphorylation sites in PDGF β-receptor juxtamembrane and kinase insert domains, Oncogene 16 (1998) 505–515.
[16] M. David, L. Wong, R. Flavell, S.A. Thompson, A. Wells, A.C. Larner, G.R. Johnson, STAT activation by epidermal growth factor (EGF) and amphiregulin, J. Biol. Chem. 271 (1996) 9185–9188.
[17] M.L. Vignais, H.B. Sadowski, D. Watling, N.C. Rogers, M. Gilman, Platelet derived growth factor induces phosphorylation of multiple JAK family kinases and STAT proteins, Mol. Cell. Biol. 16 (1996) 1759–1769.
[18] C.S. Zong, J. Chan, D.E. Levy, C. Horvath, H.B. Sadowski, L.H. Wang, Mechanism of STAT3 activation by insulin-like growth factor I receptor, J. Biol. Chem. 275 (2000) 15099–15105.
[19] M. David, E. Petricoin 3rd, C. Benjamin, R. Pine, M.J. Weber, A.C. Larner, Requirement for MAP kinase (ERK2) activity in interferon alpha- and interferon beta-stimulated gene expression through STAT proteins, Science 269 (1995) 1721–1723.
[20] F.A. Gonzalez, D.L. Raden, R.J. Davis, Identification of substrate recognition determinants for human ERK1 and ERK2 protein kinases, J. Biol. Chem. 266 (1991) 22159–22163.
[21] Z. Wen, Z. Zhong, J.E. Darnell Jr, Maximal activation of transcription by Stat1 and Stat3 requires both tyrosine and serine phosphorylation, Cell 82 (1995) 241–250.
[22] M.M. Fung, F. Rohwer, K.L. McGuire, IL-2 activation of a PI3K-dependent STAT3 serine phosphorylation pathway in primary human T-cells, Cell. Signal. 15 (2003) 625–636.
[23] K. Yokogami, S. Wakisaka, J. Avruch, S.A. Reeves, Serine phosphorylation and maximal activation of STAT3 during CNTF signaling is mediated by the rapamycin target mTOR, Curr. Biol. 10 (2000) 47–50.
[24] P.J. Coffer, A. van Puijenbroek, B.M. Burgering, M. Klop-de-Jonge, L. Koenderman, J.L. Bos, W. Kruijer, Insulin activates Stat3 independently of p21ras-ERK and PI-3K signal transduction, Oncogene 15 (1997) 2529–2539.
[25] A.W. Cohen, T.P. Combs, P.E. Scherer, M.P. Lisanti, Role of caveolin and caveolae in insulin signaling and diabetes, Am. J. Physiol. Endocrinol. Metab. 285 (2003) E1151–E1160.
[26] P. Liu, M. Rudick, R.G.W. Anderson, Multiple functions of caveolin-1, J. Biol. Chem. 277 (2002) 41295–41298.
[27] B. Razani, S.E. Woodman, M.P. Lisanti, Caveolae: from cell biology to animal physiology, Pharmacol. Rev. 54 (2002) 431–467.
[28] P.E. Scherer, R.Y. Lewis, D. Volonte, J.A. Engelman, F. Galbiati, J. Couet, D.S. Kohtz, E. van Donselaar, P. Peters, M.P. Lisanti, MP, cell-type and tissue-specific expression of caveolin-2, J. Biol. Chem. 272 (1997) 29337–29346.
[29] P.E. Scherer, T. Okamoto, M. Chun, I. Nishimoto, H.F. Lodish, M.P. Lisanti, Identification, sequence and expression of caveolin-2 defines a caveolin gene family, Proc. Natl. Acad. Sci. U. S. A. 93 (1996) 131–135.
[30] K. Das, R.Y. Lewis, P.E. Scherer, M.P. Lisanti, The membrane-spanning domains of caveolins-1 and -2 mediate the formation of caveolin hetero-oligomers, J. Biol. Chem. 274 (1999) 18721–18728.
[31] H. Kwon, K. Jeong, Y. Pak, Identification of pY19-caveolin-2 as a positive regulator of insulin-stimulated actin cytoskeleton-dependent mitogenesis, J. Cell. Mol. Med. doi:10.1111/j.1582-4934.2008.00391.
[32] H. Lee, D.S. Park, X.B. Wang, P.E. Scherer, P.E. Schwartz, M.P. Lisanti, Src-induced phosphorylation of caveolin-2 on tyrosine 19, J. Biol. Chem. 277 (2002) 34556–34567.
[33] X.B. Wang, H. Lee, F. Capozza, S. Marmon, F. Sotgia, J.W. Brooks, R. Campos-Gonzalez, M.P. Lisanti, Tyrosine phosphorylation of caveolin-2 at residue 27: differences in the spatial and temporal behavior of phospho-cav-2 (pY19 and pY27), Biochemistry 43 (2004) 13694–13706.
[34] S. Kim, Y. Pak, Caveolin-2 regulation of the cell cycle in response to insulin in Hirc-B fibroblast cells, Biochem. Biophys. Res. Commun. 330 (2005) 88–96.
[35] Y. Pak, C.R. Paule, Y.D. Bao, L.C. Huang, J. Larner, Insulin stimulates the biosynthesis of chiro-inositol-containing phospholipids in a rat fibroblast line expressing the human insulin receptor, Proc. Natl. Acad. Sci. U. S. A. 90 (1993) 7759–7763.
[36] E.M. Hwang, D.G. Kim, B.J. Lee, J. Choi, E. Kim, N. Park, D. Kang, J. Han, W.S. Choi, S.G. Hong, J.Y. Park, Alternative splicing generates a novel non-secretable cytosolic isoform of NELL2, Biochem. Biophys. Res. Commun. 353 (2007) 805–811.
[37] T. Bowman, R. Garcia, J. Turkson, R. Jove, STATs in oncogenesis, Oncogene 19 (2000) 2474–2488.
[38] J.E. Darnell Jr, Validating Stat3 in cancer therapy, Nat. Med. 11 (2005) 595–596.
[39] M.C. Kwon, B.K. Koo, J.S. Moon, Y.Y. Kim, K.C. Park, N.S. Kim, M.Y. Kwon, M.P. Kong, K.J. Yoon, S.K. Im, Crif1 is a novel transcriptional coactivator of STAT3, EMBO J. 27 (2008) 642–653.